



ELSEVIER

Journal of Organometallic Chemistry 517 (1996) 53–62

Journal
of Organometallic
Chemistry

Alkyne complexes of copper(I)
(1,1,1,5,5,5-hexafluoro-2,4-pentanedionato): syntheses and
characterization of (η^2 -bis(trimethylsilyl)acetylene) copper(I) (hfac),
(μ - η^2 -bis(trimethylsilyl)acetylene) bis(copper(I) (hfac)) and a series
of (η^2 -alkyne) Cu(hfac) complexes

Pascal Doppelt¹, Thomas H. Baum^{2,*}

IBM Almaden Research Center, 650 Harry Road, San Jose, CA 95120-6099, USA

Received 31 July 1995; in revised form 1 December 1995

Abstract

The reaction of Cu_2O with 1,1,1,5,5,5-hexafluoro-2,4-pentanedione (Hhfac) in the presence of alkynes results in the formation of (η^2 -alkyne) Cu(hfac). When using bis(trimethylsilyl)acetylene (BTMSA), both a mononuclear compound BTMSACu(hfac) (**1**) and a dinuclear complex BTMSA(Cu(hfac))₂ (**2**) can be isolated; each complex was characterized by X-ray crystallography, IR, ¹H and ¹³C NMR spectroscopies. In **1**, the BTMSA ligand is η^2 bonded parallel to the Cu (β -diketonate) plane, the trimethylsilyl groups are cis bent away from copper with small angles of deformation ($\theta_{\text{CCSi}} = 157$ and 171°) and the $\text{C}\equiv\text{C}$ bond distance is 1.17 Å. In **2**, two BTMSACu(hfac) planes with a dihedral angle of 105.8° are observed. The intramolecular Cu–Cu distance is only 2.800 Å and the central axis of BTMSA is situated perpendicular to the Cu–Cu vector. A series of η^2 -alkyne Cu(hfac) were synthesized and characterized by NMR and IR spectroscopy.

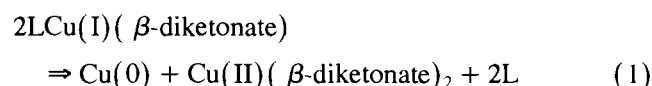
Keywords: Copper; Chemical vapor deposition; Alkyne complexes; Carbon 13; Crystal structure; Trimethylsilyl; NMR

1. Introduction

Chemical vapor deposition (CVD) processes are increasingly important for depositing conformal films and for filling high-aspect ratio vias in VLSI multi-level interconnects. The electrical resistivity of the interconnects may limit device performance, and thus low resistivity metals become increasingly desirable [1]. CVD processes for the deposition of low resistivity metals, such as gold, copper, and silver, are essential. However, to achieve gas-phase deposition, volatile metal precursors which decompose to high-purity films are required.

Previous research from our laboratory [2] and several others [3–5] has demonstrated the potential of Lewis-

base stabilized copper(I) β -diketonate complexes as copper CVD precursors. The reactive copper(I) β -diketonate moiety may be ligated with phosphines or unsaturated organics, such as alkenes, dienes and alkynes, to obtain an assortment of precursors with different physico-chemical properties. The deposition of pure copper films from the Cu(I) precursors results from a thermally-induced disproportionation reaction, shown in Eq. (1):



Using alkyne–copper complexes [6,7] the rapid deposition of high quality copper was observed; this makes these compounds of interest for further study. During the course of CVD experiments using alkyne–copper(I) hfac precursors (Hhfac = (1,1,1,5,5,5-hexafluoro-2,4-pentanedione)), we observed a chemical transformation of the precursor in the bubbler; at temperatures between 45 and 65 °C, a less-volatile solid species was formed

* Corresponding author.

¹ Permanent address: ESPCI (CNRS URA 429), 10 rue Vauquelin, 75231 Paris Cedex 05, France.

² Present address: Advanced Technology Materials, 7 Commerce Drive, Danbury, CT 06810, USA.

with time. It was believed that this chemical transformation resulted in the production of a dinuclear complex with μ - η^2 -alkyne bonding. Although this type of bonding is common in transition metal complexes [8] and in other copper(I) complexes [9], no dinuclear copper species containing a β -diketonate ligand has been reported to date. In this paper, we report the synthesis and characterization of a μ - η^2 -bis(trimethylsilyl)acetylene bis(copper(I) hexafluoroacetylacetonate), (BTMSA)-(Cu(I)hfac)₂. For comparison, we also report the X-ray crystal structure of the corresponding mononuclear complex. Lastly, IR and NMR spectral data of a series of η^2 -alkyne-Cu(hfac) complexes are reported.

2. Experimental

2.1. General procedures

All of the starting materials were commercially available and used as-received. Each synthesis was carried out under nitrogen. IR spectra were obtained using an IBM Instruments IR44 single beam spectrometer. Spectra of the 'free' unsymmetrical alkynes were obtained in a KBr solution cell with CCl₄, neat on KBr plates or in a KBr pellet. In the case of the symmetrically substituted alkynes, the literature value for the alkyne stretch ($\nu_{C=C}$) was used for comparison. The spectrum for each alkyne-copper(I) complex was obtained in a manner analogous to that used for the 'free' alkyne to enable a direct comparison. ¹H and ¹³C NMR spectra were determined on a Bruker Instrument 250 or 300 MHz spectrometer. The purified compounds were dissolved in a deuterated solvent (CDCl₃, Aldrich, 99%) to a concentration of roughly 10⁻² M. The free alkynes were dissolved in the same solvent and to roughly the same molar concentration. This procedure minimizes spectral shifts associated with concentration effects, thereby providing a realistic comparison of copper coordination spectral shifts. It should be noted, however, that spectral shifts may be dependent upon the solvent used in the analyses. Therefore, we used CDCl₃ throughout the NMR analysis and spectral shifts reported herein pertain specifically to this solvent system.

2.2. Syntheses

The syntheses of bis(trimethylsilyl)acetylene copper(I) (1,1,1,5,5,5-hexafluoro-2,4-pentanedionato), BTMSACu(hfac) (1), and other alkyne-copper(I)(hfac) complexes were carried out in one step following a previously described procedure [3b,6]. BTMSACu(hfac) was recrystallized from dichloromethane to obtain crystals suitable for an X-ray analysis, m.p. 49 °C; IR (thin film): 2964(w), 1941(C≡C, w), 1640(s), 1552(m), 1476(m), 1265(s), 1255(s), 1208(s), 1150(s), 1101(m),

848(s), 799(m), 743(s), 706(m), 671(m) cm⁻¹. ¹H NMR (CDCl₃, T = 298 K): 6.08 (s, 1H), 0.28 ppm (s, 18H). ¹³C NMR: 178.0 (q, 34 Hz, C=O), 117.8 (q, 286 Hz, CF₃), 113.2 (s, C≡C), 89.5 (s, CH), -0.3 ppm (s, SiCH₃). All other alkyne complexes were synthesized by the same procedure using commercially available alkynes (Aldrich or Wiley Organic).

Synthesis of bis(trimethylsilyl)acetylene bis(copper(I)-(1,1,1,5,5,5-hexafluoro-2,4-pentanedionato)), BTMSA(Cu(hfac))₂ (2), was carried out in a three-neck round-bottom flask charged with 5.5 g (38 mmol) of Cu₂O (Aldrich), 3 g (18 mmol) of bis(trimethylsilyl)acetylene (BTMSA) (Aldrich) and 50 ml of spectroscopic grade dichloromethane. 1,1,1,5,5,5-Hexafluoroacetylacetonate (14.7 g, 70 mmol, Aldrich) was added dropwise to the stirred solution and stirred for an additional 30 min upon completion. Excess Cu₂O was removed by filtration and the solvent was distilled off. The recovered solid was a 1:1 mixture of 1 and 2 which was sublimed at 70 °C under a vacuum of 1 Torr; after 30 min, the majority of the sublimate was the mononuclear complex (1). The sublimation residue was dissolved in dichloromethane, from which the dinuclear complex (2) was isolated after two crystallizations at -78 °C. The purified compound (12% non-optimized yield) consisted of yellow plates that were used for X-ray analysis; m.p. 113 °C; IR (solid): 2965(w), 1739(C≡C, w), 1640(s), 1554(m), 1525(m), 1474(s), 1346(w), 1256(s), 1209(s), 1149(s), 1100(w), 840(s), 799(m), 763(m), 671(s) cm⁻¹; ¹H NMR (CDCl₃, T = 220 K): 6.11 (s, 1H), 0.35 ppm (s, 10H). ¹³C NMR: 178.2 (q, 35 Hz, C=O), 117.6 (q, 285 Hz, CF₃), 89.9 (s, CH), 103.6 (s, C≡C), -0.4 ppm (s, SiCH₃). Anal. Found: C, 30.37; H, 2.93; Cu 18.04; F, 31.48; Si, 8.46. C₁₈H₂₀Cu₂F₁₂O₄Si₂. Calc.: C, 30.38; H, 2.83; Cu, 17.86; F, 32.04; Si, 7.89%.

2.3. X-ray structural analyses

Two series of crystals were submitted to Molecular Structure Corp., Woodlands, TX (USA), for X-ray analysis. The analyses were performed on a Rigaku AFC5R diffractometer with graphite monochromated Cu K α radiation ($\lambda = 1.54178$ Å) and a 12 kW rotating anode generator. The data were collected at -120 °C for 1 and 23 °C for 2 using the ω -2 θ scan technique to a maximum 2 θ value of 120.2°. ω scans of several intense reflections were made prior to data collection; ω had an average width at half-height of 0.23° and a takeoff angle of 6.0°. The weak reflections ($I < 35.0\sigma(I)$) were rescanned (minimum of 3 rescans) and the counts were accumulated to assure good counting statistics. Stationary background counts were recorded on each side of the reflection. The ratio of peak counting time to background counting time was 2:1. The diameter of the incident beam collimator was 0.5 mm

and the crystal to detector distance was 400.0 mm. All calculations were performed using the TEXSAN crystallographic software package of Molecular Structure Corp. The crystallographic data for **1** and **2** are summarized in Table 1.

2.3.1. (BTMSA)Cu(hfac) (**1**)

Cell constants and an orientation matrix for data collection were obtained from a least squares refine-

ment; the setting angles of 20 carefully centered reflections in the range of $40.7 < 2\theta < 57.9^\circ$ correspond to an orthorhombic cell with the dimensions: $a = 9.874(2)$, $b = 21.924(3)$, $c = 9.698(1)$ Å, $V = 2099.4(6)$ Å³. For $Z = 4$ and a formula weight of 446.28, the calculated density is 1.412 g cm⁻³. The successful solution and refinement of the structure leads to a space group of $P2_12_12_1$ (No. 19) with $R = 0.089$ and $R_w = 0.092$. Of the 1620 reflections, 1394 were unique ($R_{\text{int}} = 0.094$).

Table 1
Crystallographic data

Crystal data		
Empirical formula	CuC ₁₃ H ₁₉ F ₆ O _{2.33} Si ₂	Cu ₂ C ₁₈ H ₂₀ F ₁₂ O ₄ Si ₂
Formula weight	446.28	711.60
Crystal color, habit	yellow, plate	yellow, plate
Crystal dimensions (mm ³)	0.25 × 0.20 × 0.04	0.25 × 0.20 × 0.40
Crystal system	orthorhombic	monoclinic
No. reflections used for unit cell determination (2θ range)	20 (40.7–57.9°)	25 (40.0–51.4°)
ω scan peak width at half-height	0.40	0.19
Lattice parameters		
<i>a</i> (Å)	9.874 (2)	10.880 (2)
<i>b</i> (Å)	21.924 (3)	16.715 (2)
<i>c</i> (Å)	9.698 (1)	16.874 (1)
<i>V</i> (Å ³)	2099.4 (6)	2987.1 (5)
Space group	$P2_12_12_1$ (No. 19)	$P2_1/n$ (No. 14)
<i>Z</i> value	4	4
<i>D</i> _{calc} (g cm ⁻³)	1.412	1.582
<i>F</i> ₀₀₀	906	1416
μ(Cu K α) (cm ⁻¹)	31.13	34.42
Intensity measurements		
Diffractometer	Rigaku AFC5R	Rigaku AFC5R
Radiation	Cu K α (λ = 1.54178 Å)	Cu K α (λ = 1.54178 Å)
Temperature (°C)	-120	23
Attenuators	Zr foil (factors; 3.8,13.4,47.7)	Zr foil (factors; 3.8,13.4,47.7)
Take-off angle (deg)	6.0	6.0
Detector aperture (mm)	6.0 horizontal 6.0 vertical	6.0 horizontal 6.0 vertical
Crystal to detector distance (cm)	40	40
Scan type	ω-2θ	ω-2θ
Scan rate in ω	8.0 (3 rescans)	8.0 (3 rescans)
Scan width (deg)	1.26 + 0.35tan θ	1.26 + 0.35tan θ
2θ _{max} (deg)	199.1	120.1
No. of reflections measured		
Total	1620	4616
Unique	1394	4343
<i>R</i> _{int}	0.094	0.060
Corrections		
	Lorentz-polarisation	Lorentz-polarisation
	Absorption	Absorption (trans. factors: 0.81–1.00)
	(trans. factors: 0.86–1.23)	Decay (-16% decline)
	Decay (-23% decline)	Secondary extinction coefficient: 0.61927 × 10 ⁻⁶)
Structure solution and refinement		
Structure solution	direct methods	direct methods
Refinement	full-matrix least squares	full-matrix least squares
Function minimized	Σw(<i>F</i> _o - <i>F</i> _c) ²	Σw(<i>F</i> _o - <i>f</i> _c) ²
Least squares weights	4 <i>F</i> _o ² /σ ² (<i>F</i> _o ²)	4 <i>F</i> _o ² /σ ² (<i>F</i> _o ²)
p-factor	0.01	0.01
Anomalous dispersion	all non-hydrogen atoms	all non-hydrogen atoms

Table 1 (continued)

No. observations ($I > 3.00\sigma(I)$)	673	1306
No. variables	109	197
Reflection/parameter ratio	6.17	6.63
Residuals, R ; R_w	0.089; 0.092	0.076; 0.079
Goodness of fit indicator	4.68	3.88
Max shift/error in final cycle	0.00	0.00
Maximum peak in final difference map ($e^- \text{ \AA}^{-3}$)	0.82	0.53
Minimum peak in final difference map ($e^- \text{ \AA}^{-3}$)	-0.58	-0.43

Relevant expressions are as follows, where F_o and F_c represent the observed and calculated structure factor amplitude. Function minimized was $w(|F_o| - |F_c|)^2$, where $w = (s(F))^{-2}$. $R = \sum(|F_o| - |F_c|) / \sum |F_o|$. $R_w = [\sum w(|F_o| - |F_c|)^2 / \sum |F_o|^2]^{1/2}$.

The intensities of three representative reflections were measured after every 150 reflections and show an average decline in intensity of 24%. A fifth-order polynomial was used to correct for this decay. The combination of decay and disorder of the CF_3 groups indicates that only limited data were obtained. The structure was solved by SHELXS-86. Only the Cu and the Si atoms were refined anisotropically. The remaining ordered atoms were refined isotropically. The parameters refined for each rigid body used to model the CF_3 groups were: the center of mass (three parameters), three orientational angles and an overall isotropic B . The hydrogen atoms were included in the structure calculation in idealized positions ($d_{\text{C-H}} = 0.95 \text{ \AA}$). The final cycle of full-matrix least squares refinement was based upon 673 observed reflections and 109 variable parameters. There was a large residual density peak in the Fourier difference output which was not associated with the molecule and was assigned to be a partially-occupied water molecule, O(3). Atomic coordinates are given in Table 2, and selected bond lengths and angles in Tables 3 and 4 respectively. The remaining data are presented as supplementary material. The atom labeling scheme is shown in Fig. 1.

2.3.2. $\text{BTMSA}(\text{Cu}(\text{hfac}))_2$ (2)

Cell constants and an orientation matrix for data collection were obtained from a least squares refinement using the angles of 25 carefully centered reflections in the range of $40.0 < 2\theta < 51.4^\circ$ and correspond to a monoclinic cell with the dimensions: $a = 10.880(2)$, $b = 16.715(2)$, $c = 16.874(1) \text{ \AA}$, $V = 2987.1(5) \text{ \AA}^3$. For $Z = 4$ and a formula weight of 711.60, the calculated density is 1.582 g cm^{-3} . The successful solution and refinement of the structure lead to a space group of $P2_1/n$ (No 14) with $R = 0.076$ and $R_w = 0.079$. In this case, of the 4616 reflections, 4343 were unique ($R_{\text{int}} = 0.060$). Here, a decay of 16% was measured and a linear correction factor was applied to the data to account for this phenomenon. All four CF_3 groups are rotationally disordered. This disorder was modeled using rigid bodies with fixed geometries (bond lengths

and angles). Each CF_3 was represented by two rigid bodies, each with 50% occupancy. Parameters refined for each rigid body were the center of the mass and three orientation angles. One of the two SiMe_3 groups is also disordered. Rather than using rigid bodies for the refinement of this region, which would preclude anisotropic refinement of the Si atom, each of the disordered carbons was split into two half-occupied sites. All six 'half-carbons' were allowed to refine isotropically. The two Cu, two Si and four O atoms were refined anisotropically. All non-methyl carbon atoms were refined isotropically. Hydrogen atoms were placed according to geometry on ordered carbons. The final cycle of the full-matrix least squares refinement was based upon 1606 observed reflections and 197 variable parameters. The nine hydrogens associated with the disordered SiMe_3 group were omitted from the structure. The ordered carbon atoms were not refined anisotropically owing to a poor data to parameter ratio. Atomic coordinates are given in Table 5, and selective bond lengths and angles in Tables 6 and 7 respectively. The remaining data are presented as supplementary material. The atom labeling scheme is shown in Fig. 2.

3. Results and discussion

3.1. Syntheses

During recent CVD experiments using (η^2 -alkyne) $\text{Cu}(\text{I})(\text{hfac})$ precursors, a less volatile compound was formed in the bubbler along with copper metal. When the alkyne was 3-hexyne, the liquid precursor [6] was transformed into a yellow crystalline solid with time. The IR of this solid displayed a well-defined band at 1722 cm^{-1} that was absent in the IR spectrum of the starting compound. Isolation of the new compound was attempted, but rapid decomposition occurred in solution even at low temperatures. This unstable solid was thought to be a dinuclear species, in which the alkyne bridges two copper(I) centers in a 'butterfly' geometry. To positively prove this hypothesis, we used BTMSA,

Table 2
Positional parameters and B_{eq} for BTMSACu(hfac) (1)

Atom	x	y	z	B_{eq}
Cu(1)	0.8541(5)	0.2622(2)	0.7480(8)	2.4(2)
Si(1)	1.027(1)	0.1542(5)	0.924(1)	2.7(6)
Si(2)	0.678(1)	0.1564(5)	0.573(1)	2.8(6)
O(1)	0.963(2)	0.323(1)	0.848(2)	2.4(5)
O(2)	0.751(2)	0.326(1)	0.660(2)	3.4(6)
O(3)	0.9377	0.2363	0.2912	5.0(2)
C(1)	0.769(4)	0.381(2)	0.681(3)	2.3(9)
C(2)	0.868(4)	0.411(1)	0.757(6)	3.3(7)
C(3)	0.948(3)	0.377(2)	0.829(3)	1.9(8)
C(6)	0.807(4)	0.174(2)	0.715(4)	2.4(9)
C(7)	0.897(4)	0.179(1)	0.792(4)	2.0(9)
C(8)	1.020(4)	0.072(2)	0.945(5)	5(1)
C(9)	0.983(4)	0.192(4)	1.098(5)	6(1)
C(10)	1.197(5)	0.183(2)	0.826(5)	11(2)
C(11)	0.667(6)	0.077(2)	0.555(6)	10(2)
C(12)	0.517(4)	0.189(2)	0.634(4)	5(1)
C(13)	0.744(5)	0.192(2)	0.403(6)	9(2)
H(1)	0.8753	0.4548	0.7506	3.7
H(2)	0.9328	0.0599	0.9717	6.4
H(3)	1.0414	0.0530	0.8572	6.4
H(4)	1.0853	0.0591	1.0102	6.4
H(5)	1.0513	0.1815	1.1664	6.1
H(6)	0.9859	0.2359	1.0887	6.1
H(7)	0.8983	0.1800	1.1299	6.1
H(8)	1.2737	0.1732	0.8825	13.8
H(9)	1.2054	0.1607	0.7412	13.8
H(10)	1.1920	0.2244	0.8097	13.8
H(11)	0.6314	0.0584	0.6325	11.2
H(12)	0.6031	0.0685	0.4768	11.2
H(13)	0.7507	0.0602	0.5284	11.2
H(14)	0.5253	0.2324	0.6422	5.2
H(15)	0.4468	0.1805	0.5686	5.2
H(16)	0.4928	0.1724	0.7204	5.2
H(17)	0.8359	0.1756	0.3828	10.4
H(18)	0.6892	0.1797	0.3263	10.4
H(19)	0.7508	0.2341	0.4071	10.4
C(4)	0.668(3)	0.425(1)	0.590(3)	5.0(6)
F(1)	0.654(4)	0.478(2)	0.654(4)	5.0(6)
F(2)	0.548(3)	0.401(2)	0.569(4)	5.0(6)
F(3)	0.728(3)	0.434(2)	0.471(3)	5.0(6)
C(4A)	0.659(4)	0.422(2)	0.586(4)	9(1)
F(1A)	0.558(5)	0.430(2)	0.672(4)	9(1)
F(2A)	0.616(6)	0.392(2)	0.477(5)	9(1)
F(3A)	0.706(5)	0.475(2)	0.547(6)	9(1)
C(5)	1.063(5)	0.413(2)	0.929(5)	7(1)
F(4)	1.143(7)	0.437(3)	0.835(5)	7(1)
F(5)	1.134(7)	0.379(2)	1.012(7)	7(1)
F(6)	1.007(6)	0.457(3)	1.000(7)	7(1)
C(5A)	1.046(2)	0.4184(9)	0.925(2)	4.9(5)
F(4A)	1.168(3)	0.398(3)	0.899(3)	4.9(5)
F(5A)	1.016(3)	0.409(3)	1.055(3)	4.9(5)
F(6A)	1.040(3)	0.477(1)	0.899(3)	4.9(5)

an alkyne bearing strongly electron-donating groups, to synthesize a dinuclear copper(I) β -diketonate. Using BTMSA, we successfully isolated a dinuclear analog by direct synthesis. For a 4:1 Cu to alkyne ratio the equilibrium (Eq. (3)) shifts towards the dinuclear species in the synthesis. Although a mixture of **1** and **2** was obtained, their separation was realized by a difference

Table 3
Selected intramolecular distances involving the non-hydrogen atoms as determined by X-ray crystallographic analysis of BTMSACu(hfac) (1)

Atoms	Distance (Å)	Atoms	Distance (Å)
Cu(1)–O(1)	1.97(2)	Si(1)–C(8)	1.82(4)
Cu(1)–O(2)	1.92(3)	Si(1)–C(9)	1.93(5)
Cu(1)–C(6)	2.02(3)	Si(1)–C(10)	2.03(5)
Cu(1)–C(7)	1.92(3)	Si(2)–C(6)	1.92(4)
C(6)–C(7)	1.17(5)	Si(2)–C(11)	1.75(5)
Si(1)–C(7)	1.90(4)	Si(2)–C(12)	1.83(4)
		Si(2)–C(13)	1.94(5)

Estimated standard deviations in the least significant figure are given in parentheses.

Table 4
Selected intramolecular bond angles involving the non-hydrogen atoms as determined by X-ray crystallographic analysis of BTMSACu(hfac) (1)

Atoms	Angle (deg)	Atoms	Angle (deg)
O(1)–Cu(1)–O(2)	91(1)	Cu(1)–C(6)–Si(2)	117(2)
O(1)–Cu(1)–C(6)	149(1)	Cu(1)–C(6)–C(7)	68(2)
O(1)–Cu(1)–C(7)	115(1)	Si(2)–C(6)–C(7)	171(3)
O(2)–Cu(1)–C(6)	120(1)	Cu(1)–C(7)–Si(1)	125(2)
O(2)–Cu(1)–C(7)	155(1)	Cu(1)–C(7)–C(6)	78(2)
C(6)–Cu(1)–C(7)	34(1)	Si(1)–C(7)–C(6)	157(3)
C(7)–Si(1)–C(8)	110(2)	Cu(1)–O(1)–C(3)	122(2)
C(6)–Si(2)–C(11)	108(2)	Cu(1)–O(2)–C(1)	124(2)

Estimated standard deviations in the least significant figure are given in parentheses.

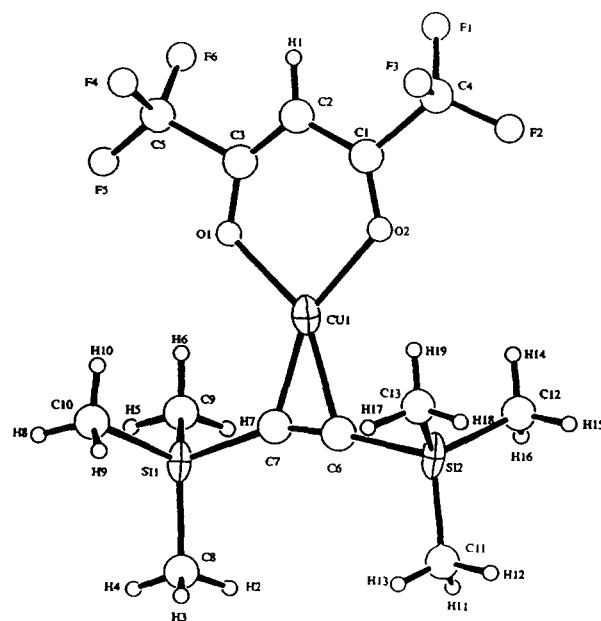


Fig. 1. ORTEP view of the mononuclear complex BTMSACu(hfac) (1).

in volatility. The solid dinuclear complex is stable at $-25\text{ }^{\circ}\text{C}$ for weeks. In solution, it is stable for several hours at $-25\text{ }^{\circ}\text{C}$, but rapidly decomposes at room temperature. Decomposition leads to the mononuclear complex, metallic copper and Cu(II)(hfac)_2 (Eq. (2)), as expected for a copper(I) disproportionation reaction:

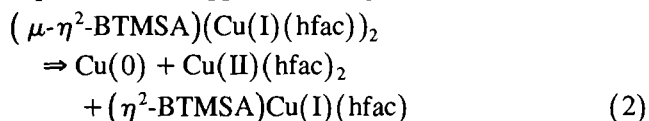


Table 5
Positional parameters and B_{eq} for $\text{BTMSA}(\text{hfac})\text{Cu}_2$ (2)

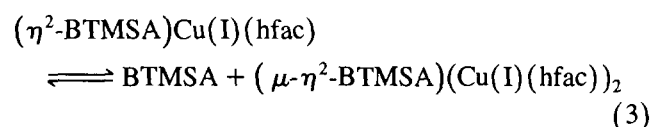
Atom	x	y	z	B_{eq}
Cu(1)	0.0530(3)	0.0467(2)	0.7015(2)	6.8(2)
Cu(2)	0.2926(3)	0.1171(2)	0.7299(2)	6.6(2)
Si(1)	0.0465(6)	0.2473(4)	0.7093(5)	8.3(4)
Si(2)	0.2106(7)	0.0492(4)	0.9017(4)	8.5(4)
O(1)	-0.071(1)	0.0529(7)	0.5987(7)	6.9(7)
O(2)	0.027(1)	-0.0683(7)	0.7022(8)	7.3(8)
O(3)	0.450(1)	0.0582(8)	0.7641(8)	7.6(8)
O(4)	0.344(1)	0.1733(8)	0.6423(8)	7.5(8)
C(1)	-0.133(2)	0.008(1)	0.559(1)	5.9(5)
C(2)	-0.130(2)	-0.071(1)	0.571(1)	6.0(5)
C(3)	-0.049(2)	-0.130(1)	0.648(1)	5.7(5)
C(6)	0.168(2)	0.095(1)	0.796(1)	5.4(5)
C(7)	0.128(2)	0.149(1)	0.746(1)	5.5(5)
C(8)	0.139(2)	0.328(1)	0.776(1)	10.0(7)
C(9)	-0.115(3)	0.241(2)	0.725(2)	13.0(9)
C(10)	0.053(2)	0.259(2)	0.603(2)	12.2(8)
C(11)	0.041(5)	0.037(3)	0.931(3)	11(1)
C(12)	0.284(4)	-0.052(2)	0.896(2)	7(1)
C(13)	0.292(4)	0.127(2)	0.973(3)	8(1)
C(11A)	0.132(6)	0.105(4)	0.972(4)	15(2)
C(12A)	0.171(5)	-0.050(3)	0.908(3)	11(2)
C(13A)	0.390(5)	0.073(3)	0.947(3)	13(2)
C(14)	0.450(2)	0.165(1)	0.629(1)	6.6(6)
C(15)	0.550(2)	0.117(1)	0.671(1)	6.9(6)
C(16)	0.539(2)	0.069(1)	0.732(1)	6.8(6)
H(1)	-0.1822	-0.1062	0.5385	7.2
H(2)	0.6285	0.1186	0.6549	8.2
H(3)	0.2263	0.3171	0.7837	12.0
H(4)	0.1158	0.3284	0.8267	12.0
H(5)	0.1199	0.3782	0.7497	12.0
H(6)	0.1385	0.2579	0.5988	14.6
H(7)	-0.1119	0.2358	0.7818	15.7
H(8)	-0.1601	0.2887	0.7054	15.7
H(9)	-0.1572	0.1963	0.6969	15.7
H(10)	0.0078	0.2167	0.5718	14.6
H(11)	0.0161	0.3088	0.5832	14.6
C(4)	-0.225(1)	0.037(1)	0.4772(9)	9.0(4)
F(1)	-0.180(2)	0.091(1)	0.446(1)	9.0(4)
F(2)	-0.247(2)	-0.021(1)	0.423(1)	9.0(4)
F(3)	-0.331(2)	0.056(2)	0.497(1)	9.0(4)
C(4A)	-0.233(1)	0.0355(9)	0.4784(9)	8.5(4)
F(1A)	-0.188(2)	0.019(1)	0.415(1)	8.5(4)
F(2A)	-0.339(2)	-0.0031(1)	0.473(1)	8.5(4)
F(3A)	-0.252(2)	0.113(1)	0.481(1)	8.5(4)
C(5)	-0.055(2)	-0.1976(9)	0.664(1)	9.4(4)
F(4)	-0.116(2)	-0.235(2)	0.598(1)	9.4(4)
F(5)	0.058(1)	-0.229(1)	0.688(2)	9.4(4)
F(6)	-0.117(2)	-0.205(1)	0.721(1)	9.4(4)
C(5A)	-0.052(2)	-0.198(1)	0.664(1)	12.9(6)
F(4A)	-0.011(3)	-0.215(2)	0.742(1)	12.9(6)

Table 5 (continued)

Atom	x	y	z	B_{eq}
F(5A)	-0.165(2)	-0.229(2)	0.638(2)	12.9(6)
F(6A)	0.025(3)	-0.227(2)	0.623(2)	12.9(6)
C(17)	0.472(1)	0.216(1)	0.5540(9)	8.9(4)
F(7)	0.591(1)	0.235(1)	0.565(1)	8.9(4)
F(8)	0.438(2)	0.172(1)	0.488(1)	8.9(4)
F(9)	0.403(2)	0.281(1)	0.546(2)	8.9(4)
C(17A)	0.474(2)	0.225(1)	0.557(1)	15.2(7)
F(7A)	0.369(2)	0.231(2)	0.501(2)	15.2(7)
F(8A)	0.505(3)	0.294(2)	0.591(2)	15.2(7)
F(9A)	0.565(3)	0.200(2)	0.523(2)	15.2(7)
C(18)	0.665(1)	0.024(1)	0.780(1)	10.1(4)
F(10)	0.638(2)	-0.050(1)	0.798(2)	10.1(4)
F(11)	0.746(2)	0.021(1)	0.733(1)	10.1(4)
F(12)	0.715(2)	0.063(1)	0.847(1)	10.1(4)
C(18A)	0.658(2)	0.013(1)	0.771(1)	14.4(6)
F(10A)	0.657(3)	-0.012(2)	0.845(1)	14.4(6)
F(11A)	0.650(3)	-0.048(2)	0.722(1)	14.4(6)
F(12A)	0.763(3)	0.052(2)	0.773(2)	14.4(6)

Estimated standard deviations in the least significant figure are given in parentheses.

We also observed an equilibrium between the mononuclear and dinuclear BTMSA complexes, since very pure mononuclear complex produces dinuclear complex when heated to $60\text{ }^{\circ}\text{C}$ in a glass ampoule, as shown in Eq. (3):



At the present time, it is possible that this equilibrium occurs for the other alkyne-copper(I) complexes reported herein, but definitive analytical data have not been obtained.

3.2. X-ray analyses

The X-ray crystallographic molecular structures of the two complexes are displayed in Figs. 1 and 2. The

Table 6
Selected intramolecular distances involving the non-hydrogen atoms as determined by X-ray crystallographic analysis of $\text{BTMSA}(\text{hfac})\text{Cu}_2$ (2)

Atoms	Distance (\AA)	Atoms	Distance (\AA)
Cu(1)–Cu(2)	2.800(4)	Si(1)–C(7)	1.90(2)
Cu(1)–O(1)	1.96(1)	Si(1)–C(8)	1.88(2)
Cu(1)–O(2)	1.94(1)	Si(1)–C(9)	1.84(3)
Cu(1)–C(6)	1.96(2)	Si(1)–C(10)	1.83(3)
Cu(1)–C(7)	1.97(2)	Si(2)–C(6)	1.90(2)
Cu(2)–O(3)	1.94(1)	Si(2)–C(11)	2.03(6)
Cu(2)–O(4)	1.94(1)	Si(2)–C(12)	1.88(4)
Cu(2)–C(6)	1.98(2)	Si(2)–C(13)	1.84(4)
Cu(2)–C(7)	1.94(2)	Si(2)–C(11A)	1.86(7)
C(6)–C(7)	1.25(3)	Si(2)–C(12A)	1.73(6)
		Si(2)–C(13A)	1.96(5)

Estimated standard deviations in the least significant figure are given in parentheses.

Table 7

Selected intramolecular bond angles involving the non-hydrogen atoms as determined by X-ray crystallographic analysis of BTMSA(Cu(hfac))₂ (2)

Atoms	Angle (deg)	Atoms	Angle (deg)
Cu(2)–Cu(1)–O(1)	121.2(4)	Cu(1)–C(6)–Cu(2)	90.4(8)
Cu(2)–Cu(1)–O(2)	123.1(4)	Cu(1)–C(6)–Si(2)	125(1)
Cu(2)–Cu(1)–C(6)	45.1(6)	Cu(1)–C(6)–C(7)	72(1)
Cu(2)–Cu(1)–C(7)	43.9(6)	Cu(2)–C(6)–Si(2)	123.4(9)
O(1)–Cu(1)–O(2)	94.1(5)	Cu(2)–C(6)–C(7)	70(1)
O(1)–Cu(1)–C(6)	147.6(7)	Si(2)–C(6)–C(7)	155(2)
O(1)–Cu(1)–C(7)	110.9(6)	Cu(1)–C(7)–Cu(2)	91.4(9)
O(2)–Cu(1)–C(6)	118.0(7)	Cu(1)–C(7)–Si(1)	120.3(9)
O(2)–Cu(1)–C(7)	155.0(6)	Cu(1)–C(7)–C(6)	71(1)
C(6)–Cu(1)–C(7)	37.0(8)	Cu(2)–C(7)–Si(1)	125(1)
Cu(1)–Cu(2)–O(3)	124.0(4)	Cu(2)–C(7)–C(6)	73(1)
Cu(1)–Cu(2)–O(4)	119.6(4)	Si(1)–C(7)–C(6)	155(2)
Cu(1)–Cu(2)–C(6)	44.5(6)	O(3)–Cu(2)–C(7)	151.0(7)
Cu(1)–Cu(2)–C(7)	44.7(6)	O(4)–Cu(2)–C(6)	151.0(7)
O(3)–Cu(2)–O(4)	94.8(6)	O(4)–Cu(2)–C(7)	114.0(7)
O(3)–Cu(2)–O(6)	114.2(7)	C(6)–Cu(2)–C(7)	37.1(8)
		C(7)–Si(1)–C(8)	106.1(9)

Estimated standard deviations in the least significant figure are given in parentheses.

pertinent bond lengths and angles are respectively listed in Tables 3 and 4 for **1**, and Tables 6 and 7 for **2**. The structure of **1** is imprecise owing to sublimation or decomposition of the crystal, even at low temperature (–120 °C). Nevertheless, some interesting structural features can be deduced. First, the structure is similar to that of (η^2 -butyne)Cu(I)(hfac) [6]. The copper–alkyne–carbon bond distances are unequal, being 2.02(3) and 1.92(3) Å. The two Si–C≡C angles are different (157(3) and 171(3)°), but not far from the linear geometry of the ‘free’ alkyne. This distortion may result from crystal lattice packing or from preferential orbital overlap between the Cu d_{xy} and unoccupied Si d orbitals on one trimethylsilyl (TMS) group. The C≡C distance is 1.17(5) Å in the complex and not appreciably elongated

relative to ‘free’ 2-butyne (1.211 Å) [10]. The extent of π back-bonding in η^2 -alkyne–metal complexes may be inferred from the C≡C bond lengthening and the extent of alkyl deformation (C≡C–R angles) from the linear geometry in the ‘free’ alkyne [11]. Based upon the relatively small perturbation of BTMSA in **1**, we expect alkyne–copper bonding to be dominated by σ bonding (electron donation from the alkyne to the copper center). Also, no significant intermolecular interactions were detected in the crystal.

The molecular structure of **2** consists of two BTMSA(Cu(hfac)) planes with a dihedral angle of 105.8° (Fig. 2). Since dinuclear complex formation requires the orbital overlap of both the p_x and p_y orbitals of the alkyne with two copper(I) centers, one would expect the dihedral angle to be 90°. The intramolecular Cu–Cu distance is short (2.800(4) Å), but the internuclear forces of the two d^{10} centers may be responsible for the increased dihedral angle relative to the expected orthogonal geometry [12]. It should be noted that shorter Cu–Cu distances have been reported in the literature [12,13]. In **2**, the main axis of the BTMSA ligand is situated perpendicular to the Cu–Cu vector, according to Hoffmann’s classification of alkyne complexes [8]. The C≡C bond distance (1.25(3) Å) is slightly elongated relative to **1**, but shorter than that reported for other dinuclear transition metal complexes [9]. The observed alkyl deformation angle ($\theta_{CCSi} = 155(2)^\circ$) is larger than the average deformation angle in **1** (164°). Both the longer C≡C bond distance and the slightly larger alkyl deformation angles (Si–C≡C) indicate increased π back-bonding in **2** in relation to **1**. As also noted for **1**, no significant intermolecular interactions could be detected in the crystal of **2**.

3.3. Lewis base bonding in η^2 -alkyne Cu(I) β -diketonates

The dominant bonding mode in the alkyne–metal complexes may be evaluated by vibrational spectroscopy (IR) and NMR spectral shifts. Here, we report the ¹H and ¹³C NMR spectra for a series of alkyne–copper(I) hfac complexes and compare the chemical shifts of the ‘free’ alkyne with the copper coordinated alkyne. This provides a qualitative measure of the dominant alkyne–copper bonding mode [14]. As previously reported, either the σ or π bonding contribution can dominate during overlap of the alkyne $p\pi$ orbital with the empty 4s or filled d_{xy}/d_{xz} orbitals of the copper(I) center. As demonstrated for alkene copper(I) triflates [15] and copper(I) β -diketonates [2c], the bonding mode may depend upon the chemical identity of the Lewis base, as well as the ancillary ligand.

The NMR chemical shift changes $\Delta\delta$ in the proton spectra of the alkyne complexes are determined primarily by local diamagnetic effects and neighboring group

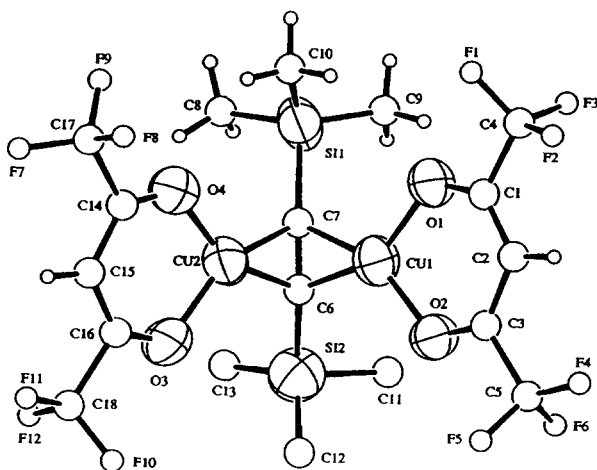


Fig. 2. ORTEP view of the dinuclear complex BTMSA(Cu(hfac))₂ (**2**).

anisotropy [16]. For the protons α to the alkyne, deshielding occurs, upon coordination to copper(I), owing to alkyne deformation. For example, the alkyl substituents on the alkyne are cis bent away from the copper(I) center and out of the linear axis of the alkyne ($C\equiv C$) π electron cloud (p_x and p_y). The degree of alkyne deformation is directly related to the extent of π back-bonding during metal–alkyne bonding [17]. For 3-hexyne and (η^2 -3-hexyne)Cu(hfac), deshielding of both the α ($-CH_2-$) and β ($-CH_3$) protons are observed. The 1H $\Delta\delta$ for a series of alkynes and alkyne–Cu(I) hfac complexes are listed in Table 8. In all cases, deshielding of the hydrogens (protons) on the α carbon atom (α to the alkyne moiety) are observed. The $\Delta\delta$ varies from +0.14 ppm (in TMS substituted alkynes) to +0.51 ppm in several of the alkyne complexes. Larger chemical shift changes (greater than +2.0 ppm) are noted for terminal alkynes, as noted for (3,3-dimethyl-1-butyne)Cu(hfac) and (TMS-acetylene)Cu(hfac). As stated above, the observed $\Delta\delta$ results primarily from alkyl deformation out of the linear axis of the alkyne electron cloud ($C\equiv C$) after complexation to copper(I). Although proton shielding can result from dominant π back-bonding and an increased electron density at the alkyne, shielding (upfield shift) is not observed in any of the proton spectra of alkyne–Cu(hfac) complexes.

In general, ^{13}C NMR spectral changes are more useful for evaluating the dominant bonding mode in alkyne–metal complexes. The local paramagnetic contribution (σ_p) is primarily responsible for $\Delta\delta$ in the carbon spectra [18]. The local paramagnetic contribution is influenced by perturbations in the electron density, the multiple bond order and/or a change in the average

Table 8

Experimentally measured chemical shift and coordination chemical shift ($\Delta\delta$) for 1H NMR of the 'free' alkyne and the alkyne Cu(I)hfac

Alkyne	$\delta_{X-C=C}$	$\delta_{X-C=CCu(I)}$	$\Delta\delta$
2-Butyne	1.71	2.13	+0.42
3,3-Dimethyl-1-butyne	2.04/1.22	4.33/1.38	+2.29/+0.16
2-Pentyne	2.01/1.72	2.52/2.17	+0.51/+0.45
2-Hexyne	2.07/1.75	2.49/2.19	+0.22/+0.44
3-Hexyne	2.09	2.54	+0.45
4-Methyl-2-hexyne	2.23/1.73	2.67/2.16	+0.44/+0.43
2-Heptyne	2.48/1.71	2.52/2.18	+0.04/+0.47
3-Heptyne	2.08/1.46	2.53/1.66	+0.45/+0.20
6-Methyl-3-heptyne	2.10/1.97	2.55/2.43	+0.45/+0.46
4-Octyne	2.08	2.48	+0.40
TMSA	2.35/0.17	4.78/0.33	+2.43/+0.16
TMS-2-Propyne	1.84/0.11	2.27/0.27	+0.43/+0.16
BTMSA	0.14	0.28	+0.14
BTMSA ^b	0.14	0.35	+0.19

The proton chemical shift is for hydrogens on the α carbon (relative to the alkyne moiety) or in the β position for TMS-substituted alkynes. Spectra are referenced to the residual protons in $CDCl_3$ at 7.24 ppm. Negative signs indicate upfield shifts (shielded) and positive signs indicate downfield shifts (deshielded).

^a TMS = $-Si(CH_3)_3$. ^b Dinuclear BTMSA(Cu(hfac))₂.

Table 9

Experimentally determined chemical shift and coordination chemical shift ($\Delta\delta$) obtained from ^{13}C NMR of the 'free' alkyne and the alkyne Cu(I)hfac

Alkyne ^a	$\delta_{C=C}$	$\delta_{C=CCu(I)}$	$\Delta\delta$
2-Butyne	74.5	81.1	+6.6
3,3-Dimethyl-1-butyne	66.4/93.2	70.6/105.5	+4.2/+12.3
2-Pentyne	74.46/80.6	81.3/87.7	+6.3/+7.1
4,4-Dimethyl-2-pentyne	73.7/87.8	81.1/96.4	+7.4/+8.6
2-Hexyne	75.4/79.2	82.1/86.0	+6.6/+6.8
3-Hexyne	80.8	87.9	+7.1
4-Methyl-2-hexyne	75.1/83.7	82.0/91.3	+6.9/+7.6
2-Heptyne	75.1/79.2	81.9/86.2	+6.8/+7.0
3-Heptyne	79.3/81.7	86.2/88.7	+6.9/+7.0
6-Methyl-3-heptyne	78.3/82.4	85.2/89.2	+6.9/+6.8
3-Octyne	79.4/81.4	86.3/88.4	+6.9/+7.0
4-Octyne	80.1	86.5	+6.4
Diphenylacetylene	89.4	95.1	+5.7
TMSA	90.1/93.0	94.8/95.7	+4.7/+2.7
TMS-2-propyne	83.7/102.9	84.5/107.2	+0.8/+4.3
BTMSA	113.7	113.2	-0.50
BTMSA ^b	113.2	103.6	-10.2

The spectra were referenced to the carbon signal in the $CDCl_3$ triplet centered at 77.0 ppm. Negative signs indicate upfield shifts (shielded) and positive signs indicate downfield shifts (deshielded).

^a TMS = $-Si(CH_3)_3$. ^b Dinuclear BTMSA(Cu(hfac))₂.

electronic excitation energy [19]. The magnitude of the $\Delta\delta$ equals the summation of the individual magnitudes for each variable. Given the complexity of these variables [20], the copper–alkyne bond can only be evaluated in a qualitative sense from the NMR spectral shifts. Concurrently, the multiple bond order may be evaluated by the vibrational spectra (IR or Raman) or X-ray crystallographic analysis of the alkyne–copper complexes.

If we assume the alkyne to be a two electron donor (η^2), then ^{13}C chemical shift changes are greatly simplified and identical to the analysis for alkene–copper(I) bonding [2c,15]. For both π and σ bonding to copper(I) hfac, the $\Delta\delta$ for the alkyne carbons will always result in shielding of the alkyne carbons, unless the alkyne electron density decreases owing to dominant σ bonding. Therefore, in the case of dominant σ bonding, deshielding of the alkyne carbons will be observed [14]. The alkyne carbons are deshielded by +7.1 ppm and the α carbons ($-CH_2-$) are deshielded by +3.3 ppm in (3-hexyne)Cu(hfac). In Table 9, the alkyne-carbon $\Delta\delta$ are given for a series of alkyne–copper(I) hfac complexes. Deshielding of the alkyne carbons is observed in nearly every alkyne–copper(I) hfac complex, except when the alkyne is BTMSA, as in 1 and 2.

In the case of (η^2 -butyne)Cu(hfac) [6] and (η^2 -diphenylacetylene)Cu(hfac) [3b], the NMR spectral shifts can also be compared with the literature X-ray crystallographic data. The X-ray crystal structures indicate dominant σ bonding based upon the $C\equiv C$ bond length and small deformation angles. In essence, the alkynes are

relatively unperturbed when coordinated to Cu(I)hfac. For the ^{13}C NMR $\Delta\delta$ obtained in this work, small deshielding shifts of +6.6 and +5.7 ppm are measured for the two compounds respectively (Table 9). Therefore, the NMR data are consistent with the crystallographic data and we can conclude that the alkyne is a two electron donor (η^2) with dominant σ bonding (electron donation from the alkyne to the copper center).

As stated above, shielding is only observed in the ^{13}C NMR spectra of **1** and **2**. A small shielding shift indicates an increased electron density at the alkyne carbons from π back-bonding. In fact, shielding or small deshielding values are noted for all of the TMS-substituted alkynes (i.e. trimethylsilyl acetylene (TMSA) and trimethylsilyl propyne (TMSP) Cu(hfac)) when compared with the other alkyne–Cu(hfac) $\Delta\delta$ values (Table 9). We believe this indicates that the TMS group(s) directly influence(s) the alkyne–copper bonding mode via electronic effects. An independent spectroscopic analysis of TMS-substituted acetylenes concluded that positive inductive polarization and electron back-donation occurred from both alkyne π orbitals (p_x and p_y) to silicon [21]. This alters the electronic properties of the alkyne and, ultimately, its bonding to the Cu(I) center. As noted in the NMR data, the π back-bonding contribution is increased for TMS-substituted alkyne–Cu(hfac) complexes. Interestingly, the X-ray crystal structures of BTMSACu(hfac) and BTMSA–(Cu(hfac))₂ indicate only minor alkyne bond lengthening and relatively small alkyl deformation angles. Although a direct d–d interaction between Si and Cu is possible, this is unlikely based upon the separation length observed in the crystal structures. Nevertheless, the electronic effects of the TMS group(s) clearly alter(s) the dominant bonding mode in the Cu(hfac) complexes, as demonstrated by the ^{13}C NMR spectral changes ($\Delta\delta$).

Vibrational spectroscopy (IR and Raman) may also be used to evaluate alkyne–metal bonding [22]. A comparison of the ‘free’ alkyne stretch frequency ($\nu_{\text{C}\equiv\text{C}}$) to that in the Cu(hfac) complexes can be obtained. Literature values were used for the C \equiv C stretch frequency for the ‘free’ symmetrical alkynes [23]. Alkyne–transition-metal bonding usually decreases the bond order of the alkyne (from sp to sp²), thereby lowering the frequency of the alkyne stretch ($\Delta\nu$) [17,22]. The magnitude of this change is directly related to the alkyne bond order and nuclearity of the complex. Large frequency changes (equal to or greater than 400 cm⁻¹) have been reported for complexes with large π back-bonding contributions [24]. For the (alkyne)Cu(hfac) complexes reported herein, relatively small frequency changes ($\Delta\nu \sim 200$ cm⁻¹) are observed, as shown in Table 10. Of special note, however, is the larger vibrational change ($\Delta\nu = 368$ cm⁻¹) observed for BTMSA(Cu(hfac))₂; **2** also displayed shielding of the alkyne carbons by NMR, and

Table 10

Vibrational frequencies for the alkyne stretch ($\nu_{\text{C}\equiv\text{C}}$) for the ‘free’ alkynes and the alkyne–Cu(hfac) complexes

Alkyne ^a	$\nu_{\text{C}\equiv\text{C}}$	$\nu_{\text{C}\equiv\text{CCu(I)}}$	$\Delta\nu$
2-Butyne	2233	2057	176
2-Hexyne	2270	2052	218
3-Hexyne	2231	2061	170
2-Heptyne	2235	2050	185
3-Heptyne	2233	2041	192
4-Octyne	2234	2044	190
Diphenylacetylene	2217	1987	230
TMSA	2037	1868	169
TMS-2-propyne	2184	2021	163
BTMSA	2107	1941	166
BTMSA ^b	2107	1739	368

Both IR and literature Raman spectral data were used to determine the frequency of the ‘free’ alkyne. A comparison of the experimentally measured frequency for the Cu(I)hfac complex with the ‘free’ alkyne provides a frequency shift ($\Delta\nu$) which is relatively small. A larger frequency change is observed for the dinuclear complex BTMSA(Cu(hfac))₂.

^a TMS = –Si(CH₃)₃. ^b Dinuclear BTMSA(Cu(hfac))₂.

the combined analytical data supports either increased π back-bonding or dinuclearity of the complex. In contrast, all of the other alkyne Cu(hfac) species display smaller $\Delta\nu$, dominant σ bonding and mononuclear copper structures.

The potential of using a volatile, dinuclear copper precursor for CVD was of interest towards facilitating the disproportionation of two copper(I) centers on a heated surface and depositing a copper film. However, attempts to utilize this approach have met with limited success as a result of the decreased volatility and the decreased thermal stability of the dinuclear complex. This work also demonstrates, however, that dinuclear (μ - η^2 -alkyne)(Cu(hfac))₂ complexes can be formed when using the (η^2 -alkyne)(Cu(hfac)) for Cu CVD. Low bubbler temperatures, or shifting the equilibrium towards the mononuclear precursor, are preferred when using these materials for the CVD of copper films.

4. Conclusions

The synthesis and X-ray crystallographic molecular structure of a mononuclear and dinuclear copper(I)(hfac) stabilized with BTMSA are reported. The mononuclear complex (**1**) is comparable with other reported alkyne–copper(I)hfac structures; the alkyne is η^2 bonded, parallel to the Cu(I) β -diketonate plane. The dinuclear complex (**2**) consists of two BTMSACu(hfac) planes with a dihedral angle of 105.8°. The structural information on the BTMSA ligand obtained via X-ray, IR and NMR spectral analyses, suggest that greater π back-bonding occurs in **2**, but that the alkyne is relatively unaffected by coordination to two copper(I) centers. As a consequence, the metal–alkyne bond is fairly weak, resulting

in two BTMSA complexes of 'limited' stability. For **2**, we observe the stability to be decreased relative to **1**.

5. Supplementary material available

Tables of the complete distances and angles in the complexes (hfac)CuBTMSA and ((hfac)Cu)₂BTMSA are available. Ordering information is given on any current masthead page.

Acknowledgments

We are grateful to the IBM Corporation and the CNRS (France) and to the DRET (DGA, France, grant no. 93-1197) for partial financial support. The authors also thank M. Sherwood (IBM) for the low temperature NMR measurement.

References

- [1] M. Small and D. Pearson, *IBM J. Res. Dev.*, **34** (1990) 858.
- [2] (a) T.H. Baum, C.E. Larson and S.K. Reynolds, US Patent 5 096 737, 1992; US Patent 5, 220, 044 (1993). (b) S.K. Reynolds, C.J. Smart, E.M. Baren, T.H. Baum, C.E. Larson and P.J. Brock, *Appl. Phys. Lett.*, **59** (1991) 2332. (c) T.H. Baum, C.E. Larson and G. May, *J. Organomet. Chem.*, **425** (1992) 189. (d) P. Doppelt and T.H. Baum, *MRS Bull.*, **XIX** (8) (1994) 41.
- [3] (a) H.-K. Shin, K.M. Chi, M.J. Hampden-Smith, T.T. Kodas, J.D. Farr and M. Paffett, *Adv. Mater.*, **3** (1991) 246. (b) H.-K. Shin, K.M. Chi, J. Farkas, M.J. Hampden-Smith, T.T. Kodas and E.N. Duesler, *Inorg. Chem.*, **31** (1992) 424. (c) A. Jain, K.M. Chi, T.T. Kodas, M.J. Hampden-Smith, J.D. Farr and M.F. Paffett, *Chem. Mater.*, **3** (1991) 199. (d) H.-K. Shin, K.M. Chi, M.J. Hampden-Smith, T.T. Kodas, J.D. Farr and M.F. Paffett, *Adv. Mater.*, **3** (1991) 246.
- [4] R. Kumar, F.R. Fronczek, A.W. Maverick, W.G. Lai and G.L. Griffen, *Chem. Mater.*, **4** (1992) 533.
- [5] J.A.T. Norman, A.K. Hochberg, D.A. Roberts, P.N. Dyer and B.A. Muratore, *IEEE VLSI Multilevel Interconnect. Conf. Symp. Proc.*, 1991, p. 123. J.A.T. Norman, B.A. Muratore, P.N. Dyer, D.A. Roberts and A.K. Hochberg, *J. Phys. (Paris)*, **IV** (1991) C2-271. J.A.T. Norman, B.A. Muratore, P.N. Dyer, D.A. Roberts, A.K. Hochberg and L.H. Dubois, *Mater. Sci. Eng. B*, **17** (1993) 87.
- [6] T.H. Baum and C.E. Larson, *Chem. Mater.*, **4** (1992) 365. T.H. Baum and C.E. Larson, *J. Electrochem. Soc.*, **140** (1993) 154.
- [7] M.J. Hampden-Smith, T.T. Kodas, M. Paffett, J.D. Farr and H.-K. Shin, *Chem. Mater.*, **2** (1990) 636.
- [8] D.M. Hoffman, R. Hoffmann and C.R. Fisel, *J. Am. Chem. Soc.*, **104** (1982) 3858 and references cited therein.
- [9] D.L. Reger and M.F. Huff, *Organometallics*, **11** (1992) 69. D.L. Reger and M.F. Huff, *Organometallics*, **9** (1990) 2807. D.L. Reger, M.F. Huff, T.A. Wolfe and R.D. Adams, *Organometallics*, **8** (1989) 838.
- [10] E. Pignataro and B. Post, *Acta Crystallogr.*, **8** (1955) 672.
- [11] G. Gervasio, R. Rossetti and P.L. Stanghellini, *Organometallics*, **4** (1985) 1612.
- [12] K.M. Mertz, Jr. and R. Hoffmann, *Inorg. Chem.*, **27** (1977) 2120. F.A. Cotton, X. Feng, M. Matusz and R. Poli, *J. Am. Chem. Soc.*, **110** (1992) 7077. G.L. Soloveichik, O. Eisenstein, J.T. Poulton, W.E. Streib, J.C. Huffman and K.C. Caulton, *Inorg. Chem.*, **31** (1992) 3306.
- [13] S.P. Abraham, A.G. Samuelson and J. Chandrasekhar, *Inorg. Chem.*, **32** (1993) 6107.
- [14] M.J.S. Dewar, *Bull. Chem. Soc. Fr.*, **18** (1951) C79. J. Chatt and L.A. Duncanson, *J. Chem. Soc.*, (1953) 2939.
- [15] R.G. Salomon and J.K. Kochi, *J. Organomet. Chem.*, **43** (1972) C7. R.G. Salomon and J.K. Kochi, *J. Am. Chem. Soc.*, **95** (1973) 1889. R.G. Salomon and J.K. Kochi, *J. Organomet. Chem.*, **64** (1974) 135.
- [16] J.M. Sichel and M.A. Whitehead, *Theoret. Chim. Acta*, **5** (1966) 35.
- [17] R. Mason, *Chem. Soc. Rev.*, **1** (1972) 441. R. Mason, *Nature*, **217** (1968) 543.
- [18] M. Karplus and J.A. Pople, *J. Chem. Phys.*, **38** (1963) 2803.
- [19] J.A. Pople, *Mol. Phys.*, **7** (1963) 301.
- [20] R.H.M. Dudzelaar, R.J.J.A. Timmermanns, A. Mackor and E.J. Baerends, *J. Organomet. Chem.*, **331** (1987) 397.
- [21] H. Bock and H. Seidl, *J. Chem. Soc. B*, (1968) 1158.
- [22] S. Otsuka and A. Nakamura, *Adv. Organomet. Chem.*, **14** (1976) 245. F.R. Hartley, *Angew. Chem. Int. Ed. Engl.*, **11** (1972) 596.
- [23] R.F. Kendall, *Spectrochim. Acta A*, **24** (1968) 1839. F.F. Cleveland and M.J. Murray, *J. Chem. Phys.*, **9** (1941) 390. F.F. Cleveland, M.J. Murray and H.F. Taufen, *J. Chem. Phys.*, **10** (1942) 172. G.A. Crowder and P. Blankenship, *J. Mol. Struct.*, **156** (1987) 147. H. Hiura and H. Takahashi, *J. Phys. Chem.*, **96** (1992) 8909.
- [24] U. Rosenthal, G. Oehme, V.V. Burlakov, P.V. Petrovski, V.B. Suhr and M.E. Vol'pin, *J. Organomet. Chem.*, **391** (1990) 119. B.W. Davies and N.C. Payne, *J. Organomet. Chem.*, **99** (1975) 315.